applied sciences

MDPI

Article

Selection of Posture for Time-Trial Cycling Events

Alejandra P. Polanco [1,*], Luis E. Muñoz [2], Alberto Doria [3] and Daniel R. Suarez [1]

1 School of Engineering, Pontificia Universidad Javeriana, Carrera 7 No. 40–62, 110231 Bogota, Colombia; d-suarez@javeriana.edu.co
2 Department of Mechanical Engineering, Universidad de los Andes, Carrera 1 Este No. 19A–40, 111711 Bogota, Colombia; lui-muno@uniandes.edu.co
3 Department of Industrial Engineering, University of Padova, Via Venezia, 1, 35131 Padova, Italy; alberto.doria@unipd.it
* Correspondence: alejandra.polanco@javeriana.edu.co

Received: 12 August 2020; Accepted: 14 September 2020; Published: 19 September 2020

Featured Application: Optimization of performance in time-trial cycling events through the selection of posture while considering comfort.

Abstract: Cyclists usually define their posture according to performance and comfort requirements. However, when modifying their posture, cyclists experience a trade-off between these requirements. In this research, an optimization methodology is developed to select the posture of cyclists giving the best compromise between performance and comfort. Performance was defined as the race time estimated from the power delivery capacity and resistive forces. Comfort was characterized using pressure and vibration indices. The optimization methodology was implemented to select the aerobars' height for five cyclists riding on 20-km time-trial races with different wind speed and road grade conditions. The results showed that the reduction of the aerobars' height improved the drag area (−10.7% ± 3.1%) and deteriorated the power delivery capacity (−9.5% ± 5.4%), pressure on the saddle (+16.5% ± 11.5%), and vibrations on the saddle (+6.5% ± 4.0%) for all the tested cyclists. It was observed that the vibrations on the saddle imposed the greatest constraint for the cyclists, limiting the feasible exposure time and, in some cases, modifying the result obtained if the posture was selected considering only performance. It was concluded that optimal posture selection should be performed specifically for each cyclist and race condition due to the dependence of the results on these factors.

Keywords: bicycle; comfort; performance; posture selection; aerodynamic drag; power delivery capacity; pressure; vibrations

1. Introduction

During cycling, the human body adopts a posture different from usual postures (e.g., standing, seated, reclined). The cyclists' posture is determined by their anthropometry and is limited by the bicycle geometry. The posture of the rider is relevant because it can worsen or improve the riding experience. For this reason, the modifications of posture in cycling are usually driven by the improvement of performance and comfort.

The interest of cyclists of different levels, from recreational to professional, in performance is clear, because its improvement is a common general objective when practicing sports. Aerodynamic drag and the capacity of the cyclist to deliver power are factors affecting cycling performance that are influenced by posture.

The aerodynamic drag is related to the drag area of the combination of the bicycle and cyclist, which is the product of the drag coefficient and the projected frontal area. The variation in aerodynamic drag due to changes in posture has been reported by several authors [1–6]. In general, in upright

postures the drag area is larger than in bent-forward postures. For this reason, some cyclists aim at improving their posture by reducing their drag area. Nevertheless, it has been reported that variations in posture can affect the power delivery capacity [7–13]. In general, the power output is higher in upright postures than in bent-forward postures, which is a characteristic of aerodynamically efficient postures. For this reason, there are cases in which adopting aerodynamically efficient postures can lead to an overall performance decrement.

Together with performance, cyclists also prioritize comfort when selecting their posture. Comfort in cycling is important since discomfort can lead to pain and overuse injuries, which can force the cyclist to adopt less efficient postures or stop practicing the activity temporarily. Discomfort is common in cycling because of the constraints that the bicycle imposes on the rider. The main constraints are that the whole weight of the rider is supported by three small contact areas (i.e., buttocks–saddle, hands–handlebar, and feet–pedals), and the trunk is bent forward to allow the cyclist to simultaneously remain in contact with the saddle and the handlebar. These conditions, combined with riding sessions that can be extended for hours, lead to scenarios of frequent discomfort, and possible overuse injuries (i.e., musculoskeletal disorders, compression neuropathies, joint pain, and numbness).

Comfort depends on the mental and physical state, background, and expectations of the cyclist [14,15], thus, its assessment is difficult. As a subjective variable, comfort has been registered through visual scales in which the rider selects a level of discomfort [16,17]. Other variables, such as vibrations and pressure on contact areas, have been used to objectively quantify comfort as a result of the interaction between the bicycle and the rider [18–23]. Recent studies have shown that comfort is affected by the posture of the rider [24]. Regarding pressure, it has been reported that changes in the body posture, such as the position of the hands on the handlebar [25,26] and the trunk inclination [27], affect the pressure between contact areas. Regarding vibrations, it has been reported that the hands' position and the wrists' orientation have a significant effect on the vibrations transmitted to the cyclist [19]. Although an extensive amount of information is lacking, posture is generally identified as one of the test conditions to control when studying the vibrational behavior in cycling [28].

Due to the effects of posture on the rider's performance and comfort, the selection of posture in cycling is a non-trivial process as it considers a trade-off between aerodynamic drag and power delivery capacity [11,13,29], and it should consider potential adverse effects on the rider's body. To the best knowledge of the authors, there are no reported methods for the selection of posture in cycling that consider the aerodynamic drag, power delivery capacity, vibrations transmission, and pressure on contact areas simultaneously. Although studies exist regarding the effect of posture on performance [1–13,29] and interaction [16,17,23–25,28], further exploration is needed. This is mainly because the information available was obtained with different methodologies and for different body postures. For this reason, the results from these studies cannot be directly compared.

This study presents an optimization methodology for the selection of posture considering comfort and performance. The methodology is implemented for cyclists riding in different aerobars' postures for individual time-trial races. The optimal posture is selected considering the specific characteristics of each bicycle and cyclist and the road and environment conditions. Aerobars postures were chosen for the implementation as they are designed to optimize aerodynamics [30]. Nevertheless, it is usual for the riders to experience a reduction in their power delivery capacity when riding with aerobars [11,12,29,31–33]. This type of posture is frequently associated with discomfort because the contact with the saddle is concentrated in a smaller area leading to compression of the genital area [30,34,35]. The general purpose of this study is to implement a methodology to select the posture of cyclists and to analyze the factors affecting such a selection.

2. Materials and Methods

The proposed methodology aims at selecting the posture with the best compromise between performance and comfort from a group of tested postures. For this purpose, the total race time is used to represent the overall performance, and vibrations and pressure indices are used to represent comfort.

The methodology considers characterizing the resistive forces, power delivery capacity, vibrations, and pressure in contact areas independently for each cyclist riding in each posture. Then, the posture that minimizes the total race time for a given race condition (i.e., race distance, wind speed, and road grade) and does not exceed thresholds of exposure to vibrations and pressure is selected. To analyze the factors that affect the selection of posture, the methodology was implemented for cyclists with different characteristics. The inclusion of a group of cyclists with varied characteristics allows the exploration of possible scenarios that can be found during the posture selection process. This section describes the postures, cyclists, bicycles, and race conditions included in the study. The methods adopted to characterize the performance and comfort indices, and to select the best posture, are also described.

2.1. Postures, Cyclists, and Bicycles Tested

Five cyclists voluntarily participated with their bicycles in the study. All subjects gave their informed consent for inclusion before they participated in the study. The study was conducted in accordance with the Declaration of Helsinki, and the protocol was approved by the Ethics Committee of Pontificia Universidad Javeriana (under the project identification "Effect of cyclist's posture on its performance and interaction with the bicycle" with the code DOC-ING-131-2018). Different types of riders and bicycles were included in the study with the objective of exploring the results obtained for riders and bicycles with specific characteristics. The group of cyclists was selected to include riders of both genders (four male and one female), with different ages (a male rider for each of the age categories Senior/Elite, Masters A, Masters B, and Masters C), and different anthropometrical characteristics (four classified as healthy weight and one as overweight). The common characteristics of the group of riders included in the study are that they were recreational level cyclists, had experience in road cycling, had participated in cycling or triathlon races, and had experience riding in time-trial postures with aerobars. In addition, the participants reported they had no injuries that could affect their cycling performance. Finally, considering that all of the tests of the study were performed in a city located at an altitude of 2600 m above sea level, only cyclists that were adapted to this altitude were included. This was verified to avoid possible effects of altitude on the power output of cyclists, such as those reported by Garvican-Lewis et al. [36]. To this end, it was checked that all the cyclists lived in the same city for at least five years. Table 1 summarizes the main characteristics of the cyclists that participated in the study.

Table 1. Characteristics of the riders included in the study.

	Rider 1	Rider 2	Rider 3	Rider 4	Rider 5
Mass (kg)	92	73	73	72	59
Height (m)	1.76	1.83	1.78	1.72	1.67
Body mass index (kg/m^2)	29.7	21.8	23.0	24.3	21.2
Age (years)	42	30	39	26	38
Cycling experience (years)	9	9	20	5	17
Gender	Male	Male	Male	Male	Female

The riders performed the tests with their own bicycles. For this reason, different types of bicycles, such as endurance, time trial, and aero road bicycles, of different qualities, were included in the study. The bicycles of the participants were used with the intention of obtaining results that represent the actual riding conditions of each cyclist. The use of different bicycles could affect the test results (especially power delivery capacity and pressure on contact areas) because the riders would require extensive adaptation periods to other bicycles. Table 2 presents the main characteristics of the bicycles used by each cyclist. The riders performed the tests using standard cycling equipment (i.e., cycling helmet, short sleeve cycling jersey, padded cycling shorts, and clipless pedal shoes).

Table 2. Characteristics of the bicycles used by each rider.

	Rider 1	Rider 2	Rider 3	Rider 4	Rider 5
Type	Aero	Time trial	Endurance	Time trial	Aero
Mass (kg)	10.8	9.9	11.5	10.2	10.5
Frame size [1]	55	51.5	49	48.4	52
Frame material	Carbon fiber	Carbon fiber	Aluminum	Carbon fiber	Carbon fiber
Aerobars' height fit window (mm)	55	40	55	55	55

[1] Seat tube length in millimeters.

Different variables can be set to define the posture of a cyclist when riding in aerobars. For this study, the posture of the cyclist was varied by changing the height of the aerobars. The other variables of the bicycle geometry remained constant. Two postures with different aerobars' heights were defined for the implementation of the methodology. The aerobars' heights were set at the highest and lowest configurable limits of the bicycle (namely ABh and ABl, respectively). The configurable limits of the aerobars' heights for each bicycle are presented in Table 2. Figure 1 presents the silhouettes of the cyclists in the sagittal plane riding in the tested postures.

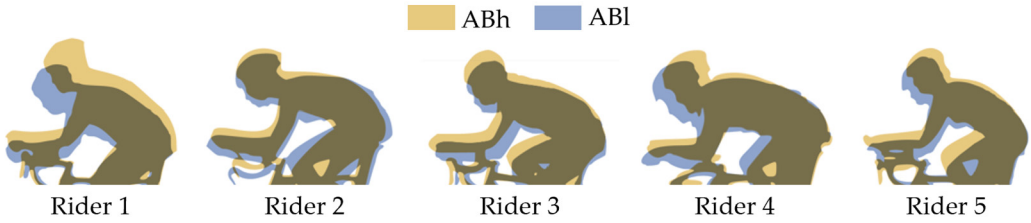

Figure 1. Postures included in the study. ABh/ABl: highest and lowest configurable limits of the aerobars' height.

2.2. Characterization Tests: Performance

The performance of each rider was characterized through variables representing resistive forces and the power delivery capacity.

2.2.1. Characterization of Resistive Forces

The aerodynamic drag characteristics were represented by the drag area (C_DA). The rolling resistance characteristics were represented by the rolling resistance coefficient (f_r). The drag area and rolling resistance coefficient were obtained using an experimental methodology based on outdoor road tests. Further details of the methodology are described by Polanco et al. [37,38]. The methodology is based on the mathematical model of the longitudinal dynamics of the rider and the bicycle presented in Equation (1).

$$M_{eq}a = \eta\left(\frac{P}{v_b}\right) - \frac{1}{2}\rho C_D A v_{w/b}^2 - mgcos(\theta)f_r - mgsin(\theta) - c_1 - c_2 v_b, \quad (1)$$

where ρ is the air density, $v_{w/b}$ is the speed of the wind relative to the bicycle, m is the mass of the bicycle and the cyclist with equipment and instrumentation, g is the gravitational acceleration, θ is the road inclination, η is the efficiency of the transmission system, P is the power delivered to the pedals, v_b is the bicycle speed, M_{eq} is the equivalent mass, a is the longitudinal acceleration, and c_1 and c_2 are constants of the equivalent bearing resistance representing the dissipation originated by the bearings of the bicycle [39].

The characterization consisted of performing several one-way rides along an outdoor test route at different constant speeds. The road grade was obtained offline from altimetry. The wind speed relative to the bicycle was measured during the tests. The power delivered by the cyclist, the bicycle speed,

and the ambient conditions were also registered on the route and averaged for each trial. Inertial and geometrical parameters of the rider with the bicycle were also measured or estimated.

The characterization of resistive forces for each rider was performed in one test day, in which both postures were characterized. The tests were performed on a straight asphalt route, with a length of 400 m, and exclusive dedication to bicycles. Each cyclist performed ten trials in each posture. The trials were performed at constant speeds between 18 and 27 km/h. The tires of all the bicycles were inflated at 8 bar. The bicycle speed was measured with a speed sensor (Speed sensor 2, Garmin, Olathe, KS, USA) located on the rear wheel hub coupled to a GPS cycle-computer (Forerunner 910XT, Garmin, Olathe, KS, USA). As a result that it is difficult for the riders to pedal at a constant speed in real conditions, small variations in the speed were expected. For this reason, the average acceleration of each trial was numerically computed using the bicycle speed and the total interval duration. The wind speed relative to the bicycle was measured with an onboard anemometer based on a pitot tube and developed specifically for this application [38]. The altimetry of the test section was measured with a topographical-grade Global Navigation Satellite System (GR-5, Topcon, Tokyo, Japan). The power delivered by the rider was measured with a power meter located in the pedals (Vector, Garmin, Olathe, KS, USA). The average temperature, relative humidity, and atmospheric pressure data were registered with a weather station (Weather meter 4500, Kestrel Instruments, Boothwyn, PA, USA) to estimate air density using the model presented by Picard et al. [40]. Figure 2 presents the setup used for the tests.

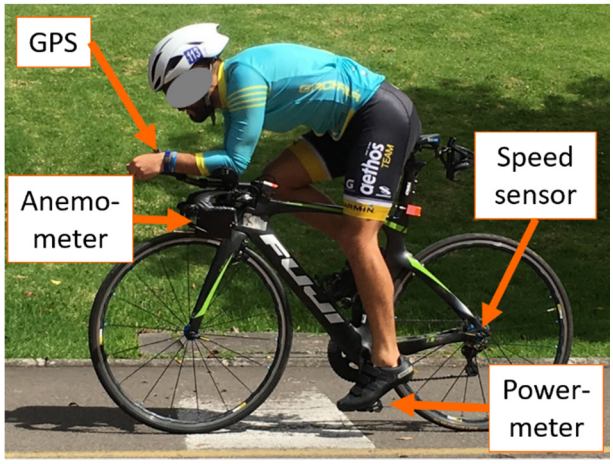

Figure 2. Setup for the characterization of the drag area and rolling resistance coefficient.

2.2.2. Characterization of Power Delivery Capacity

For the characterization of the power delivery capacity, the dependence on the time span in which the activity was performed was taken into account. This relationship between power and time has been described as a hyperbolic function in which the power output decreases as the time increases [41]. For this reason, the power delivery capacity was characterized in terms of the Functional Threshold Power (FTP) of the cyclist. The FTP is the maximum average power that a cyclist can deliver for one hour. The FTP was chosen to represent the power delivery capacity in the aerobic range.

In this study, the FTP was measured through an indoor test of self-paced pedaling. A test designed by a commercial cycling training platform was used (TheSufferFest: 4DP test, Wahoo, Atlanta, GA, USA). The test includes a time-trial test from which the FTP is obtained. The characterization of power delivery capacity for each rider was performed during two test days: one day to test each posture. A recovery period of at least one week was used between test days. The tests were performed at the same time of day to avoid possible effects of the time of day on the fatigue [42]. The riders were asked to maintain a constant diet and hydration during the execution of these tests and to refrain from performing vigorous exercise 24 h before the beginning of each test. Even though there is not a general

agreement on the influence of the menstrual cycle phase on exercise performance [43], in this study the power delivery tests with the female rider were performed during the follicular phase of the cycle.

The tests were performed indoors using a smart trainer (Kickr, Wahoo, Atlanta, GA, USA), a power meter located in the pedals (Vector, Garmin, Olathe, KS, USA), a cadence sensor (Cadence 2, Garmin, Olathe, KS, USA), a heart rate sensor (Rhythm+, Scosche, Oxnard, CA, USA), and a monitor to display the data to the cyclist. The cyclist controlled the resistance by shifting the gears. The cyclist was able to hydrate ad libitum. The average temperature and relative humidity were registered with a weather station to verify the testing conditions (Weather meter 4500, Kestrel Instruments, Boothwyn, PA, USA). Figure 3 presents the setup used for the tests.

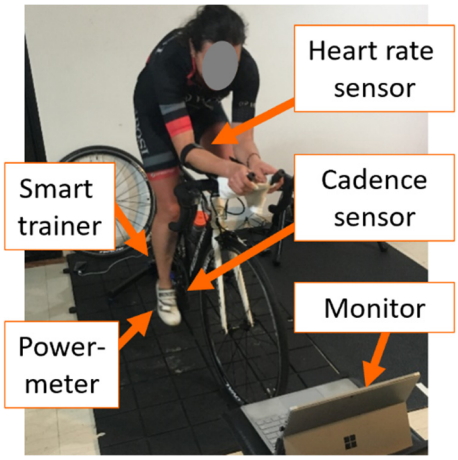

Figure 3. Setup for the characterization of the power delivery capacity.

2.3. Characterization Tests: Comfort

Comfort was quantified using indices for the pressure in the buttocks–saddle and elbows–aerobars pads contact areas, and the vibrations transmitted through the bicycle seatpost and steering tube.

2.3.1. Pressure in Contact Areas

The pressure on contact areas was defined in terms of the global average pressure (p). This index was computed in the saddle (p_S) and aerobars' elbow pads (p_{AB}). For the computation, it was considered that the pressure field was measured by sensors located on a matrix. Each sensor on the contact area registered local pressure $s_p(x, y, t)$, where x and y, respectively, are the lateral and longitudinal coordinates of the sensor, and t is the time step. The global average pressure was computed first calculating the average pressure sensed on the contact area for each time step (p_t) as in Equation (2), where A_e is the effective contact area between the bicycle and the cyclist. Then, the average over time was computed to obtain p as in Equation (3), where t_f is the total duration of the test.

$$p_t(t) = \frac{\int_{A_e} S_p(x, y, t) dA}{A_e} \tag{2}$$

$$p = \frac{\int_0^{t_f} p_t(t) dt}{t_f} \tag{3}$$

The global average pressure (p) was used in the framework of this research, because it is related to the cumulative effect on human tissues. In addition, since the position of the peak pressure varies over time, the use of the average pressure on the contact area is more suitable than a local value.

A methodology based on indoor tests to register the pressure fields in the contact areas while pedaling was used. A flexible sensing mat was used to register the pressure. The cyclist pedaled on a smart trainer at a constant cadence delivering a constant power output equal to the FTP for

1 min. The power output was held constant because it has been reported that this variable affects the pressure field in the saddle contact area [26]. The power output was defined in terms of the FTP to be representative of the power delivered by the cyclist while training or competing.

The characterization of pressure in contact areas for each rider was performed in one test day, in which both postures were characterized. A smart trainer (Kickr, Wahoo, Atlanta, GA, USA), a power meter located in the pedals (Vector, Garmin, Olathe, KS, USA), and a cadence sensor (Cadence sensor 2, Garmin, Olathe, KS, USA) were used for the tests. A pressure sensing mat (Bike saddle, Novel, Munich, Germany) with 512 capacitive sensors of 1 cm^2, located on a 32 × 16 cm^2 area, was used for measuring pressure. Figure 4 presents the setup used for the tests.

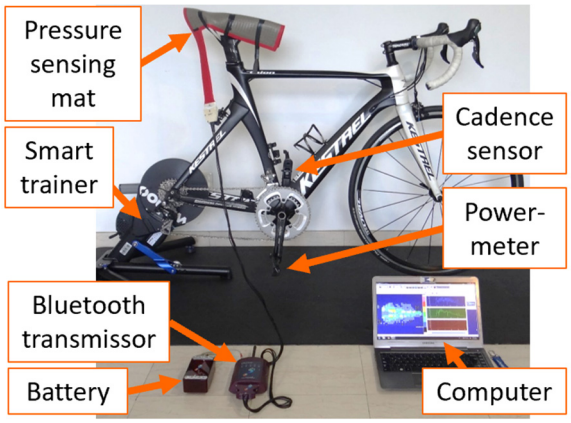

Figure 4. Setup for the characterization of the pressure in contact areas.

2.3.2. Vibrations Transmission

The vibrations transmitted through the bicycle were characterized in terms of the vibration total value (a_v) on the seatpost and the steering tube (a_{vS} and a_{vAB}, respectively). The computation was performed as in Equation (4), where a_{wx}, a_{wy}, and a_{wz} are the rms accelerations on the x, y, and z axes, respectively. The rms accelerations are defined in Equation (5), where T is the duration of the measurement in seconds, t is the time, and $a_w(t)$ is the weighted acceleration as a function of time. The subscript w is included as the accelerations were weighted by frequency to consider the human sensitivity to vibrations. For the saddle-related vibrations, the weighting curves of whole-body vibrations of the ISO 2631 [44] were used. For the aerobars-related vibrations, the weighting curves of hand-transmitted vibrations reported in the ISO 5349 [45] were used.

$$a_v = \sqrt{a_{wx}^2 + a_{wy}^2 + a_{wz}^2} \tag{4}$$

$$a_w = \sqrt{\frac{1}{T}\int_0^T a_w^2(t)dt} \tag{5}$$

The vibrations were registered during outdoor road tests with the rider pedaling at a constant speed. Triaxial accelerometers were located on the seat tube and the steering tube using clamp supports, see Figure 5. Since the clamp supports were oriented with the bicycle components, the signals were rotated to obtain the data in the vertical, lateral, and longitudinal directions.

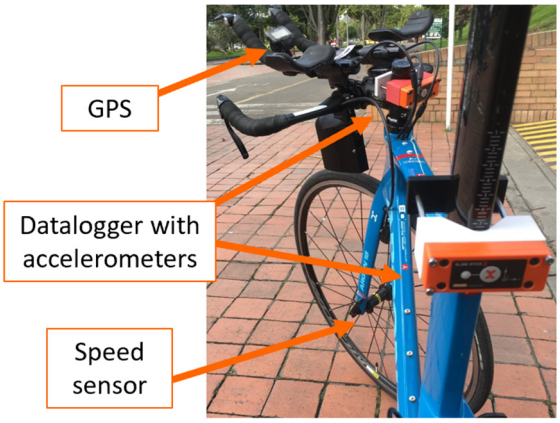

Figure 5. Setup for the characterization of vibrations transmission.

The characterization of vibration transmissions for each rider was performed in one test day, in which both postures were characterized. The vibrations were registered using data loggers with triaxial accelerometers with a sampling frequency of 5 kHz (SlamStick LOG-0002-025G-PC, Mide, Woburn, MA, USA). A GPS (Forerunner 910XT, Garmin, Olathe, KS, USA) and a speed sensor (Speed sensor 2, Garmin, Olathe, KS, USA) were used to register and display the speed to the rider in real time. The rider traveled three times at a constant speed of 25 km/h on a straight route with smooth asphalt and a length of 400 m. Figure 5 presents the setup used for the tests.

2.4. Posture Selection

This section describes the process to estimate the race time and comfort exposure thresholds and the procedure to select a posture for specific race conditions.

The posture selection was made considering the characteristics of each cyclist, each bicycle, and the race conditions. A race condition was defined by the length of the race, the road inclination, and the wind speed. In this study, multiple race conditions were studied varying the wind speed between a tailwind of 2 m/s and a headwind of 5 m/s, and the road inclination between −5% and 5%. A constant race distance of 20 km was defined for all race conditions.

2.4.1. Total Race Time

The total race time (t_r) of a given race condition was computed from the bicycle speed (v_b) and the race distance (X_r) as in Equation (6).

$$t_r = \frac{X_r}{v_b} \tag{6}$$

The bicycle speed was computed from the equation of the longitudinal dynamics of the rider and the bicycle presented in Equation (1) under the assumption of a steady-state condition leading to Equation (7).

$$\frac{1}{2}\rho C_D A(v_b + v_w)^2 + mgcos(\theta)f_r + mgsin(\theta) + c_1 + c_2 v_b = \eta\left(\frac{P_{1h}}{v_b}\right) \tag{7}$$

The computation of v_b was performed using the values of ρ, g, η, c_1, c_2 summarized in Table 3. The mass m was measured for each cyclist and bicycle. The C_DA and f_r coefficients were obtained for each posture during the aerodynamic drag characterization. The parameter P_{1h} is the capacity of the cyclist to deliver power to the pedals for intervals close to one hour. It was obtained for each posture during the power delivery capacity characterization (i.e., P_{1h} is equivalent to the FTP).

Table 3. Constants used for the computation of total race time.

Parameter	Value
Air density (ρ) (kg/m^3)	0.9
Gravitational acceleration (g) (m/s^2)	9.8
Power transmission efficiency (η) (%)	97
Equivalent bearing resistance parameter 1 (c_1) (N)	0.091
Equivalent bearing resistance parameter 2 (c_2) (N.s/m)	0.0087

For each posture, each rider, and each combination of wind speed (v_w) and road inclination (θ), the total race time t_r was calculated.

2.4.2. Exposure Thresholds

There is a relationship between the exposure time and the magnitudes of pressure and vibrations that can be sustained without adverse effects on the human body. High levels of vibration and pressure can be supported with no harm for short periods, while even relatively low magnitudes of these variables can have adverse effects if they are sustained for long periods. For this reason, exposure thresholds for these variables were defined.

Regarding pressure, the thresholds for the saddle (p_{thS}) and the aerobars (p_{thAB}) were defined using the pressure–time threshold curve for the appearance of saddle sores in humans described in Equation (8). The pressure thresholds are expressed in kPa for given exposure times t_e in hours. This curve is an approximation of the model reported by Sacks [46], which was fitted by the authors of that study to the data reported by Rescwick and Rogers [47]. It is assumed that the thresholds for the pressure in the saddle and the elbow pads are the same because there is no specific information for different contact points.

$$p_{thS} = p_{thAB} = [471.9 * t_e^{-4/3} + 11.5] * 0.13 \quad (8)$$

Regarding vibrations, the thresholds for the saddle (V_{thS}) and the aerobars (V_{thAB}) were defined using the information reported in ISO 2631 [44] for the vibrations measured close to the buttocks, and ISO 5349 [45] for the vibrations measured close to the elbows. ISO 2631 presents curves for health guidance caution zones for whole-body vibrations, while ISO 5349 mentions a threshold for an increased probability of presenting the hand–arm vibration syndrome. From these curves, it is possible to determine the thresholds of exposure by considering the equivalency between vibration exposures. This means determining the exposure time for a certain vibration level that is equivalent to a reference caution exposure time for a given acceleration. For the saddle, an exposure to vibrations of 1.2 m/s^2 for 4 h was used as a caution reference leading to the expression in Equation (9). For the aerobars, the 8-h energy-equivalent was used with an exposure threshold of 2 m/s^2, leading to the expression in Equation (10). In both equations, the vibrations thresholds are in m/s^2 and the exposure times are in hours.

$$V_{thS} = 2.4/\sqrt{t_e} \quad (9)$$

$$V_{thAB} = 5.6/\sqrt{t_e} \quad (10)$$

For each race condition, the pressure and vibrations thresholds were computed for an exposure time equal to the total race time. Then, it was verified whether the value measured for the variable during the tests exceeded the threshold value of the same condition. If one of the variables p_S, p_{AB}, a_{vS}, or a_{vAB} exceeded its corresponding threshold, the race condition was considered as not feasible. For the feasible race conditions, the percentage of the variables with respect to the corresponding thresholds was computed as described by Equations (11) to (14).

$$p_{pS} = 100 * p_S / p_{thS} \quad (11)$$

$$p_{pAB} = 100 * p_{AB} / p_{thAB} \quad (12)$$

$$V_{pS} = 100 * a_{vS} / V_{thS} \tag{13}$$

$$V_{pAB} = 100 * a_{vAB} / V_{thAB} \tag{14}$$

2.4.3. Posture Selection Model

An optimization problem was formulated to select the posture of a rider for a given race condition considering the cyclist's and bicycle's characteristics. The optimization problem was defined as finding the value of the aerobars' height (h) that minimizes the total race time for a given race condition subject to thresholds on vibrations of the seatpost and steering tube, and thresholds on the pressure in the buttocks–saddle and elbows–pads contact areas. The standard form of the optimization problem is presented in Equation (15):

$$minimize\ t_r(h) subject\ to: h \in \mathcal{H},\ g_k(h) \leq 0,\ k = 1, 2, 3, 4, \tag{15}$$

where $\mathcal{H}$ is the set of aerobars' heights under study and the restrictions g_k are as defined in Equations (16) to (19):

$$g_1(h) = p_S(h) - p_{thS}(t_r(h)), \tag{16}$$

$$g_2(h) = p_{AB}(h) - p_{thAB}(t_r(h)), \tag{17}$$

$$g_3(h) = a_{vS}(h) - V_{thS}(t_r(h)), \tag{18}$$

$$g_4(h) = a_{vAB}(h) - V_{thAB}(t_r(h)). \tag{19}$$

Two discrete options for the aerobars' height were considered to solve the optimization problem, as in Equation (20):

$$\mathcal{H} = \{h_1,\ h_2\}, \tag{20}$$

in which the values of h_1 and h_2 are defined by the lowest and highest limits of the aerobars' height according to the bicycle fit window (namely ABl and ABh, respectively). The aerobars' height difference between ABh and ABl for each bicycle is presented in Table 2.

3. Results

3.1. Characterization of Performance and Comfort Variables

The results of the performance and comfort characterizations are summarized in Table 4. The drag area, rolling resistance coefficient, power delivery capacity, global average pressure, and vibration total value obtained for each rider are presented. It can be observed that for all the riders changing from ABh to ABl led to an improvement in the drag area (−10.7% ± 3.1%), and deteriorations in the average power delivery capacity (−9.5% ± 5.4%), pressure on the saddle (+16.5% ± 11.5%), and vibrations on the saddle (+6.5% ± 4.0%). Regarding the pressure and vibrations on the aerobars, changing from ABh to ABl led to different results for the different riders without a general tendency.

The results of the variation of the drag area and power delivery capacity are in agreement with previous findings in which it is reported that, in trained male cyclists, lowering the torso angle leads to a significant reduction of physiological performance and aerodynamic gains [29]. The results of this study indicate that similar results could be obtained for female cyclists.

Table 4. Performance and comfort indices obtained from characterization.

	Posture	Rider 1	Rider 2	Rider 3	Rider 4	Rider 5
C_DA (m^2)	ABh	0.27	0.29	0.33	0.26	0.28
	ABl	0.23	0.26	0.31	0.23	0.25
f_r (-)	ABh	0.007	0.004	0.007	0.005	0.005
	ABl	0.007	0.004	0.007	0.005	0.005
P_{1h} (W)	ABh	180	233	179	228	161
	ABl	168	193	169	217	140
p_S (kPa)	ABh	52.2	26.1	15.8	39.0	13.9
	ABl	58.5	28.1	20.9	48.6	14.7
p_{AB} (kPa)	ABh	28.9	31.8	25.1	29.8	19.5
	ABl	31.5	35.8	23.4	25.9	22.0
a_{vS} (m/s^2)	ABh	2.56	2.74	3.04	2.95	3.00
	ABl	2.90	2.88	3.13	3.15	3.13
a_{vAB} (m/s^2)	ABh	4.24	5.54	4.91	4.62	4.32
	ABl	4.37	4.59	4.45	4.71	4.42

The environmental conditions and heart rate registered during the characterization tests are presented in Table 5. It is worth highlighting that the air density and wind speed are variables that affect the estimation of the drag area and rolling resistance coefficient. For this reason, the methods used for their assessment include the estimation of air density and the measurement of wind speed. The air density was computed using the temperature, relative humidity, and atmospheric pressure registered in Table 5. The air density was found to lie in a small range for all of the tests (0.88 ± 0.01 kg/m^3). The wind speed varied between the testing days between headwinds of 12.9 m/s and tailwinds of 11.9 m/s, which emphasizes the relevance of including wind speed measurements for the estimation of this variable, as described by Polanco et al. [37].

Table 5. Environmental conditions and heart rate registered during characterization tests.

Test	Variable	Posture	Rider 1	Rider 2	Rider 3	Rider 4	Rider 5
Resistive forces	Temperature (°)	ABh	18.9	29.6	22.3	17.8	21.5
		ABl	26.1	22.1	22.9	19.3	20.8
	Relative humidity (%)	ABh	59	43	59	56	56
		ABl	48	52	50	44	52
	Atmospheric pressure (kPa)	ABh	75.2	75.2	75.2	75.1	75.4
		ABl	75.2	74.9	75.2	75.1	75.4
	Maximum tailwind (m/s)	ABh	10.4	8.2	4.6	0.1	7.5
		ABl	11.9	11.5	7.4	7.0	6.5
	Maximum headwind (m/s)	ABh	10.8	12.9	10.2	7.8	5.4
		ABl	8.9	8.5	6.0	12.7	11.4
Power delivery capacity	Temperature (°)	ABh	19.8	19.2	20.0	19.8	20.8
		ABl	18.8	19.3	21.6	18.6	20.0
	Relative humidity (%)	ABh	60	59	60	60	55
		ABl	60	59	61	57	59
	Maximum heart rate (bpm)	ABh	166	184	167	180	162
		ABl	166	178	172	179	168
	Average heart rate (bpm)	ABh	138	142	136	139	135
		ABl	137	138	133	139	139

Regarding the execution of the tests for the power delivery capacity characterization, it can be observed that the temperature and relative humidity were similar in all of the testing sessions (19.8 ± 0.9 °C and 59.0 ± 1.8%, respectively). These variables were registered to verify that the ambient conditions did not present a considerable variation between the tests of each rider to avoid possible effects of temperature and humidity on performance [48,49]. It is also noted that the maximum and average heart rates of the cyclists were similar between the tests. The average heart rate difference between tests was 2.4 ± 1.8 bpm, reflecting that the cyclists had similar levels of effort in both tests.

3.2. Selection of Posture

Figure 6 provides an example of the detailed results obtained for the posture selection of rider 1. The figure presents a set of 10 subplots representing the data of ABh in the left column and the data of ABl in the right column. Each subplot presents the results for the range of v_w and θ considered. The first row of subplots presents the results associated only with performance and depicts the estimated total race times in seconds. The other rows present the results associated with contact pressures and vibrations in the saddle and aerobars in terms of percentages of the variables with respect to the corresponding exposure thresholds. Only the feasible conditions are presented. If a variable exceeds its corresponding exposure threshold for a given condition, it is not plotted.

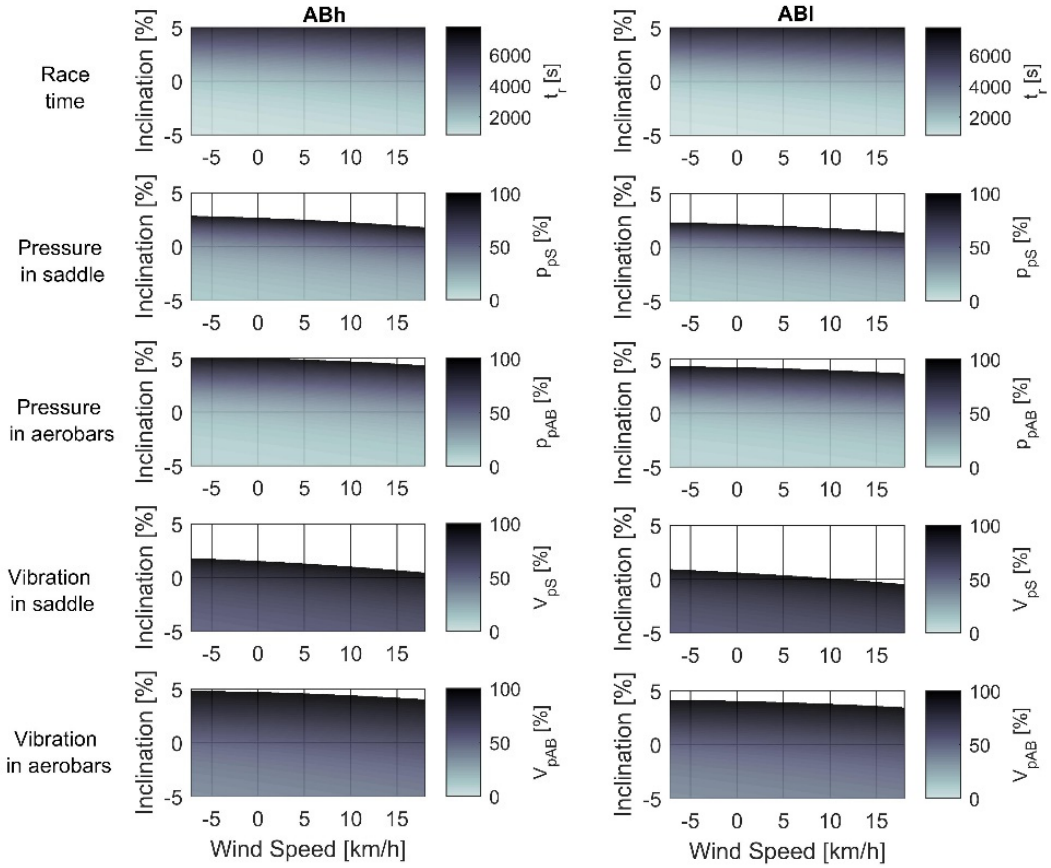

Figure 6. Detailed results obtained for the posture selection of rider 1.

The results of rider 1 show higher race times for the conditions with higher inclinations and headwinds. Congruently, as the race time increases, the time of exposure to vibrations and pressure increases, leading to smaller acceptable thresholds. For this reason, the unfeasible conditions are obtained at higher inclinations and headwinds. It can also be observed that for all of the comfort-related variables, there are unfeasible race conditions; nevertheless, the vibrations in the saddle represent the strictest constraint with more unfeasible race conditions. This means that this variable can modify the posture selection.

Figure 7 presents the selected posture of the various cyclists and bicycles in the various race conditions. The selected posture leads to the best time while satisfying all of the constraints. If the posture with the best time does not satisfy one of the constraints, then the other posture is selected. If the other posture also does not satisfy one of the constraints, then the race condition is considered as unfeasible and is not plotted. The plot presents the posture selected for each race condition using a light color when the selected posture is ABl and a dark color when it is ABh. In addition, a red dotted

line is included in the plot that represents the threshold between the zones of posture selection that would be obtained if only the race time was considered (i.e., without including comfort constraints).

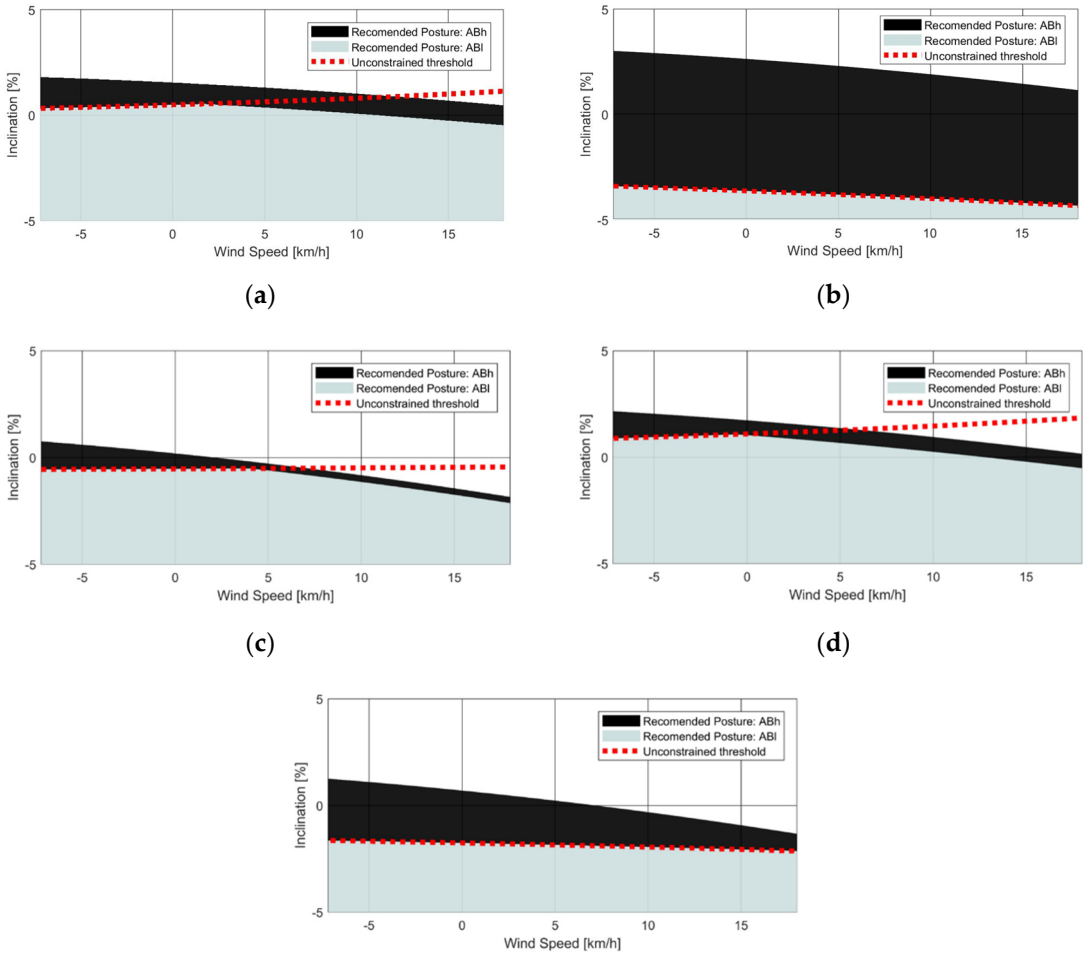

Figure 7. Posture selection results for the tested cyclists and bicycles. (**a**) Rider 1; (**b**) Rider 2; (**c**) Rider 3; (**d**) Rider 4; (**e**) Rider 5.

The comparison of the posture threshold line due to race time only (red dotted line) with the zones of posture selection (light and dark color areas) shows that only for some cyclists the dotted line corresponds with the change between the postures (i.e., Riders 2 and 5). A difference between the dotted line and the border between light and dark color areas implies that, for some race conditions, the selection of posture is modified by the constraints (i.e., vibrations or pressure thresholds). A match between the line and the shades' interface implies that the posture selection can be performed based on performance only (i.e., race time).

When considering the posture selection based only on performance (red dotted line in Figure 7), it was observed that, even if for all the riders the drag area and power delivery capacity presented the same directions of improvement and decrement (Table 4), the characteristics of the posture selection threshold were different for each rider. This means that the results of the posture selection methodology depend on the characteristics of the rider and bicycle on both postures. This phenomenon can be analyzed by rearranging Equation (7) as in Equation (21):

$$\frac{\rho C_D A (v_b + v_w)^2 v_b}{2P_{1h}} + \frac{c_2 {v_b}^2}{P_{1h}} + \frac{[mgcos(\theta) f_r + mgsin(\theta) + c_1] v_b}{P_{1h}} - \eta = 0. \quad (21)$$

Equation (21) shows that the relationship between drag area and power delivered, C_DA/P_{1h}, is relevant for the computation of the bicycle speed v_b because it multiplies the cubic and quadratic terms. For this reason, the relationship between drag area and power delivery capacity and the differences between the postures for each rider are presented in Table 6. It is worth noticing that, when this difference is positive, the performance-only selection threshold increases (i.e., Riders 1, 3, and 4). In addition, the slope of the threshold is related to the magnitude of the C_DA/P_{1h} difference. This result emphasizes the relevance of characterizing the power delivery capacity and drag area of the cyclist.

Table 6. Relationship between drag area and power delivery capacity.

	Rider 1	Rider 2	Rider 3	Rider 4	Rider 5
ABh (m^2/kW)	1.5	1.2	1.8	1.1	1.7
ABl (m^2/kW)	1.4	1.3	1.8	1.1	1.8
Difference (m^2/kW)	0.13	−0.10	0.01	0.08	−0.05

Table 7 presents the race time and the percentages of the thresholds for vibrations and pressure in saddle and aerobars for the zero-wind speed and zero-grade race condition. The table also presents the selected posture for each rider for the same race conditions. In this case, the time gains due to the posture selection vary between 14 and 97 s, with an average of 47.2 s. It is worth highlighting that these time gains are representative only for the cyclist, bicycle, and race characteristics of this example. For some cyclists, the time gains are obtained in ABl when referenced to ABh, while for others, it is vice versa. It is worth highlighting that for some cyclists ABl is an unfeasible posture because the vibration on the saddle exceeds the threshold. Congruently, the results summarized in the table reflect that the strictest constraints are related to the vibrations thresholds as the percentages of the variables are higher than those registered for pressure.

Table 7. Race time, and pressure and vibrations threshold percentages computed for a zero-wind, zero-grade race condition.

	Posture	Rider 1	Rider 2	Rider 3	Rider 4	Rider 5
t_r (s)	ABh	2095	1745	2162	1751	2032
	ABl	2063	1842	2176	1724	2098
p_{pS} (%)	ABh	40	16	13	23	10
	ABl	44	18	17	29	11
p_{pAB} (%)	ABh	23	19	20	18	14
	ABl	25	23	19	15	17
V_{pS} (%)	ABh	82	80	98	86	94
	ABl	92	86	unfeasible	91	unfeasible
V_{pAB} (%)	ABh	57	68	67	57	57
	ABl	58	58	61	58	60
Selected posture		ABl	ABh	ABh	ABl	ABh

4. Discussion

The purpose of this study was to implement a methodology for the selection of optimal time-trial postures and to analyze the factors affecting the selection. The methodology is based on the selection of the posture that leads to the best prediction of race time while meeting comfort constraints. For the implementation of the methodology, the drag area and power delivery capacity were characterized to predict the race time. In addition, the pressure in contact areas and vibrations in contact points were characterized as objective indices of comfort.

Regarding the characterization of the performance and comfort variables, from the group of cyclists measured, the cyclist with the largest loss of power delivery capacity when changing from ABh to ABl was rider 2 (17%). This participant described himself as not flexible and reported being uncomfortable when riding in ABl, which was in agreement with his power output reduction. The cyclist with the

second largest loss of power delivery capacity was rider 5 (13%), who also described herself as not flexible. On the contrary, the cyclist with the lowest loss of power delivery capacity with the change of posture was rider 4 (5%), who reported being comfortable in both postures. In agreement with Burt [34], these results highlight the relevance of flexibility of cyclists for the posture selection. Regarding the drag area, the rider with the largest difference of C_DA between the postures tested was rider 1 (15%), who reported not being comfortable in intermediate postures. This difference was expected from the visual examination of the postures in Figure 1. The cyclist with the highest drag area values was rider 3; although he was not the biggest rider among the participants, his bicycle had the lowest quality among those included in the study, which is reflected in the drag area values registered.

Regarding the selection of posture, it can be observed that the results depend on the wind speed and road inclination. This indicates that the posture selection process should consider these race conditions. It can also be observed that the results have a substantial variation for the different riders (Figure 7). This indicates that the posture selection process should be performed considering the characteristics of each rider and bicycle. These findings complement the results of Fintelman et al. [29], who noted that the optimal time-trial posture is defined considering characteristics of the rider (i.e., frontal area, physiology) and race conditions (i.e., cycling speed, course inclination, and duration). With the results of this study, the characterization of comfort and wind speed are added to the variables defining optimal time-trial posture, and the characteristics of the rider are specified as the drag area and power delivery capacity.

It is worth noting that for several race conditions, the less aerodynamic posture, ABh in this study, can be more advantageous than the aerodynamically efficient posture ABl. For example, when considering a race condition in flat terrain (i.e., zero road grade), ABh is the recommended posture at every wind speed for Riders 2, 3, and 5. Moreover, for Riders 1 and 4, the ABl posture is recommended for all of the displayed race conditions when the selection is performed based only on performance (i.e., in the area below the dotted line). Nevertheless, when the comfort constraints are considered, there is a range of wind speeds for which ABh is recommended instead of ABl. The race conditions for which ABh is recommended are found at higher headwinds. This can be seen in Figure 7 for a 0% inclination as the change from light to dark color when increasing headwind speed. The change is found at 13 km/h for rider 1 and 10.5 km/h for rider 4. This result can be counterintuitive because, at higher wind speeds, the aerodynamic drag gains relevance indicating that the more aerodynamically efficient posture ABl should be selected. Nevertheless, at higher headwinds, the race times also increase, leading to shorter pressure and vibration exposure thresholds, making ABl an unfeasible posture for some race conditions.

Another example is a race condition with no wind speed. In this case, it can be observed that for each rider there are specific road inclinations in which the recommended posture changes from ABl to ABh. It is worth noting that the road inclination of posture change for each rider is the same if the selection is performed based on performance only or considering the comfort constraints. The road inclination of posture change varied over the riders between −3.6% and 1%, meaning that for some cyclists, even on descending roads, ABh is more advantageous than ABl (see Riders 2, 3, and 5). This phenomenon occurs because the power delivery capacity of these cyclists was significantly reduced when adopting the most aerodynamic posture. Hence, unless the aerodynamic advantage compensated the power delivery reduction, ABl would not be recommended. These results highlight that a more aggressive aerodynamic posture does not necessarily lead to race time improvements and, on the contrary, it can have adverse effects on the comfort of the riders.

The results of the optimal posture selection when considering only performance permitted identifying that the relation C_DA/P_{1h}, is relevant for the computation of the race time. More specifically, the difference between the ratios of the postures under comparison has a relationship with the tendency of the performance-only selection threshold (Table 6 and Figure 7). This means that the variation of the C_DA/P_{1h} ratio when changing the posture has a strong influence on the determination of the advantageous posture.

The practical implications of the results of this study are that the optimal selection of posture should be performed considering the specific characteristics of the bicycle and the cyclist on the possible postures to be selected, and the race conditions. In particular, the power delivery capacity, aerodynamic drag, and vibrations on the saddle are characteristics of the rider that should be considered. The race distance, the road inclination, and the wind speed should be considered as well to represent the race conditions. Another practical implication is that the ratio between the drag area and the power delivery capacity has a strong influence on the overall performance of a cyclist understood as the race time when riding on a given posture. For this reason, the most aerodynamically efficient posture is not always the optimal posture.

In the framework of this study different research directions were identified. First, the results obtained in this study for performance and comfort could be further refined by including other relevant variables. For example, considering requirements associated with the bicycle stability [50,51] and pacing strategies [52,53] could be explored. Second, the methodology for the selection of posture could be implemented for a group of cyclists with homogeneous characteristics for a statistically based study. Third, the methodology could be implemented for the selection of postures by varying more than one postural parameter (e.g., variation of the saddle and aerobars' vertical and longitudinal positions and inclinations). Fourth, there are several research opportunities associated with the study of the relationship between time to exposure and potential damage caused by the pressure and vibrations in the contact points between the rider and the bicycle.

5. Conclusions

A methodology for the selection of optimal time-trial postures considering performance and comfort was implemented. The methodology considers the characterization of the performance and comfort of the rider through objective quantitative indices. The selection was performed by minimizing the race time, which was estimated using the drag area and power delivery capacity of the cyclist. The selection was constrained by thresholds associated with the riders' exposure to pressure in contact areas and vibrations.

The results show that for the tested group of riders, reducing the height of aerobars in time-trial postures results in an improvement of the drag area, and deteriorations in the average power delivery capacity, average pressure on the saddle, and vibrations on the saddle. Although these tendencies were observed, it was found that the optimal posture selection depends on the characteristics of each cyclist and bicycle, and race conditions. Regarding the characteristics of the cyclist and the bicycle, it was found that the drag area to power delivery capacity ratio and the saddle vibration of each rider in each posture govern the posture selection process. Regarding the race conditions, it was found that the posture selection depends on the longitudinal wind speed, the road inclination, and the race distance. For these reasons, the selection of posture is a non-trivial process that should consider the trade-off between the possible improvements on aerodynamic drag and the losses in power delivery capacity, and comfort on the saddle.

Author Contributions: Conceptualization, A.P.P., L.E.M., A.D., and D.R.S.; methodology, A.P.P., and L.E.M.; software, A.P.P.; validation, A.P.P.; formal analysis, A.P.P., L.E.M., A.D., and D.R.S.; investigation, A.P.P.; resources, A.P.P.; data curation, A.P.P.; writing—original draft preparation, A.P.P.; writing—review and editing, A.P.P., L.E.M., A.D., and D.R.S.; visualization, A.P.P., and L.E.M.; supervision, A.D. and D.R.S.; project administration, A.P.P.; funding acquisition, A.P.P. All authors have read and agreed to the published version of the manuscript.

Funding: This research was partially funded by the Colombian Administrative Department of Science, Technology, and Innovation (COLCIENCIAS) under grant 727-2015 and Pontificia Universidad Javeriana. The APC was funded by Pontificia Universidad Javeriana.

Conflicts of Interest: The authors declare no conflict of interest.

References

1. Barry, N.; Burton, D.; Sheridan, J.; Thompson, M.; Brown, N. Aerodynamic Performance and Riding Posture in Road Cycling and Triathlon. *Proc. Inst. Mech. Eng. Part P J. Sports Eng. Technol.* **2015**, *229*, 28–38. [CrossRef]
2. Oggiano, L.; Leirdal, S.; Saetran, L.; Ettema, G. Aerodynamic Optimization and Energy Saving of Cycling Postures for International Elite Level Cyclists. *Eng. Sport* **2008**, *7*, 597–604. [CrossRef]
3. Chabroux, V.; Barelle, C.; Favier, D. Aerodynamics of Cyclist Posture, Bicycle and Helmet Characteristics in Time Trial Stage. *J. Appl. Biomech.* **2012**, *28*, 317–323. [CrossRef] [PubMed]
4. Chowdhury, H.; Alam, F. Bicycle Aerodynamics: An Experimental Evaluation Methodology. *Sports Eng.* **2012**, *15*, 73–80. [CrossRef]
5. Jeukendrup, A.E.; Martin, J. Improving Cycling Performance. *Sports Med.* **2001**, *31*, 559–569. [CrossRef]
6. Defraeye, T.; Blocken, B.; Koninckx, E.; Hespel, P.; Carmeliet, J. Aerodynamic Study of Different Cyclist Positions: CFD Analysis and Full-Scale Wind-Tunnel Tests. *J. Biomech.* **2010**, *43*, 1262–1268. [CrossRef]
7. Egaña, M.; Green, S.; Garrigan, E.J.; Warmington, S. Effect of Posture on High-Intensity Constant-Load Cycling Performance in Men and Women. *Eur. J. Appl. Physiol.* **2006**, *96*, 1–9. [CrossRef]
8. Egaña, M.; Smith, S.; Green, S. Revisiting the Effect of Posture on High-Intensity Constant-Load Cycling Performance in Men and Women. *Eur. J. Appl. Physiol.* **2007**, *99*, 495–501. [CrossRef]
9. Emanuele, U.; Denoth, J. Influence of Road Incline and Body Position on Power-Cadence Relationship in Endurance Cycling. *Eur. J. Appl. Physiol.* **2012**, *112*, 2433–2441. [CrossRef]
10. Welbergen, E.; Clijsen, L.P. The Influence of Body Position on Maximal Performance in Cycling. *Eur. J. Appl. Physiol. Ophthalmol.* **1990**, *61*, 138–142. [CrossRef] [PubMed]
11. Ashe, M.C.; Scroop, G.C.; Frisken, P.I.; Amery, C.A.; Wilkins, M.A.; Khan, K.M. Body Position Affects Performance in Untrained Cyclists. *Br. J. Sports Med.* **2003**, *37*, 441–444. [CrossRef] [PubMed]
12. Gnehm, P.; Reichenbach, S.; Altpeter, E.; Widmer, H.; Hoppeler, H. Influence of Different Racing Positions on Metabolic Cost in Elite Cyclists. *Med. Sci. Sports Exerc.* **1997**, *29*, 818–823. [CrossRef] [PubMed]
13. Grappe, F.; Candau, R.; Busso, T.; Rouillon, J.D. Effect of Cycling Position on Ventilatory and Metabolic Variables. *Int. J. Sports Med.* **1998**, *19*, 336–341. [CrossRef] [PubMed]
14. Christiaans, H.; Bremner, A. Comfort on Bicycles and the Validity of a Commercial Bicycle Fitting System. *Appl. Ergon.* **1998**, *29*, 201–211. [CrossRef]
15. Laios, L.; Giannatsis, J. Ergonomic Evaluation and Redesign of Children Bicycles Based on Anthropometric Data. *Appl. Ergon.* **2010**, *41*, 428–435. [CrossRef]
16. Chiu, M.; Wu, H.; Tsai, N. The relationship between handlebar and saddle heights on cycling comfort. In *Human Interface and the Management of Information*; Yamamoto, S., Ed.; Springer: Berlin, Germany, 2013; pp. 12–19.
17. Chen, Y.; Liu, Y. Optimal Protruding Node Length of Bicycle Seats Determined using Cycling Postures and Subjective Ratings. *Appl. Ergon.* **2014**, *45*, 1181–1186. [CrossRef]
18. Olieman, M.; Marin-Perianu, R.; Marin-Perianu, M. Measurement of Dynamic Comfort in Cycling using Wireless Acceleration Sensors. *Procedia Eng.* **2012**, *34*, 568–573. [CrossRef]
19. Lépine, J.; Champoux, Y.; Drouet, J. Road Bike Comfort: On the Measurement of Vibrations Induced to Cyclist. *Sports Eng.* **2014**, *17*, 113–122. [CrossRef]
20. Hölzel, C.; Höchtl, F.; Senner, V. Cycling Comfort on Different Road Surfaces. *Procedia Eng.* **2012**, *34*, 479–484. [CrossRef]
21. Wu, X.; Rakheja, S.; Boileau, P. Study of Human–seat Interface Pressure Distribution under Vertical Vibration. *Int. J. Ind. Ergon.* **1998**, *21*, 433–449. [CrossRef]
22. Doria, A.; Marconi, E.; Muñoz, L.; Polanco, A.; Suarez, D. An experimental-numerical method for the prediction of on-road comfort of city bicycles. *Veh. Syst. Dyn.* **2020**, 1–21. [CrossRef]
23. Doria, A.; Marconi, E. A Testing method for the prediction of comfort of city bicycles. In Proceedings of the ASME 2018 IDETC Conference, Quebec City, QC, Canada, 26–29 August 2018. [CrossRef]
24. Polanco, A.; Suarez, D.; Muoz, L. Effect of body posture on comfort during cycling. In Proceedings of the ASME 2017 IDETC Conference, Cleveland, OH, USA, 6–9 August 2017. [CrossRef]
25. Bressel, E.; Cronin, J. Bicycle Seat Interface Pressure: Reliability, Validity, and Influence of Hand Position and Workload. *J. Biomech.* **2005**, *38*, 1325–1331. [CrossRef] [PubMed]

26. Potter, J.J.; Sauer, J.L.; Weisshaar, C.L.; Thelen, D.G.; Ploeg, H.L. Gender Differences in Bicycle Saddle Pressure Distribution during Seated Cycling. *Med. Sci. Sports Exerc.* **2008**, *40*, 1126–1134. [CrossRef]
27. De Vey Mestdagh, K. Personal Perspective: In Search of an Optimum Cycling Posture. *Appl. Ergon.* **1998**, *29*, 325–334. [CrossRef]
28. Polanco, A.; Marconi, E.; Muñoz, L.; Suárez, D.; Doria, A. Effect of Rider Posture on Bicycle Comfort. In Proceedings of the ASME 2019 IDETC Conference, Anaheim, CA, USA, 18–21 August 2019. [CrossRef]
29. Fintelman, D.M.; Sterling, M.; Hemida, H.; Li, F. The Effect of Time Trial Cycling Position on Physiological and Aerodynamic Variables. *J. Sports Sci.* **2015**, *33*, 1730–1737. [CrossRef] [PubMed]
30. Burke, E. *High-Tech Cycling*, 2nd ed.; Human Kinetics: Champaign, IL, USA, 2003.
31. Hubenig, L.; Game, A.; Kennedy, M. Effect of Different Bicycle Body Positions on Power Output in Aerobically Trained Females. *Res. Sports Med.* **2011**, *19*, 245–258. [CrossRef] [PubMed]
32. Jensen, R.; Balasubramani, S.; Brennan, G.; Burley, K.; Kaukola, D.; LaChapelle, J.; Shafat, A. Power output, muscle activity, and frontal area of a cyclist in different cycling positions. In Proceedings of the XXV ISBS Symposium, Ouro Preto, Brazil, 23–27 August 2007.
33. Charlton, J.M.; Ramsook, A.H.; Mitchell, R.A.; Hunt, M.A.; Puyat, J.H.; Guenette, J.A. Respiratory Mechanical and Cardiorespiratory Consequences of Cycling with Aerobars. *Med. Sci. Sports Exerc.* **2017**, *49*, 2578–2584. [CrossRef] [PubMed]
34. Burt, P. *Bike Fit: Optimise Your Bike Position for High Performance and Injury Avoidance*; Bloomsbury: London, UK, 2014.
35. Gemery, J.; Nangia, A.; Mamourian, A.; Reid, S. Digital Three-dimensional Modelling of the Male Pelvis and Bicycle Seats: Impact of Rider Position and Seat Design on Potential Penile Hypoxia and Erectile Dysfunction. *BJU Int.* **2007**, *99*, 135–140. [CrossRef] [PubMed]
36. Garvican-Lewis, L.A.; Clark, B.; Martin, D.; Schumacher, Y.O.; McDonald, W.; Stephens, B.; Ma, F.; Thompson, K.G.; Gore, C.J.; Menaspa, P. Impact of Altitude on Power Output during Cycling Stage Racing. *PLoS ONE* **2015**, *10*, e0143028. [CrossRef]
37. Polanco, A.; Roa, S.; Suarez, D.; Lopez, O.; Muñoz, L. Influence of wind speed and road grade on the estimation of drag area in cycling. *Sports Biomech.* **2020**. under review.
38. Polanco, A.; Fuentes, J.; Porras, S.; Castiblanco, D.; Uribe, J.; Suarez, D.; Muñoz, L. Methodology for the Estimation of the Aerodynamic Drag Parameters of Cyclists. In Proceedings of the ASME 2019 IDETC Conference, Anaheim, CA, USA, 18–21 August 2019. [CrossRef]
39. Martin, J.C.; Gardner, A.S.; Barras, M.; Martin, D.T. Modeling Sprint Cycling using Field-Derived Parameters and Forward Integration. *Med. Sci. Sports Exerc.* **2006**, *38*, 592–597. [CrossRef] [PubMed]
40. Picard, A.; Davis, R.S.; Glaser, M.; Fujii, K. Revised formula for the density of moist air (CIPM-2007). *Metrologia* **2008**, *45*, 149. [CrossRef]
41. Bergstrom, H.; Housh, T.; Zuniga, J.; Traylor, D.; Lewis, R.; Camic, C.; Schmidt, R.; Johnson, G. Responses during Exhaustive Exercise at Critical Power Determined from the 3-Min all-Out Test. *J. Sports Sci.* **2013**, *31*, 537–545. [CrossRef] [PubMed]
42. Lericollais, R.; Gauthier, A.; Bessot, N.; Sesboue, B.; Davenne, D. Time-of-day effects on fatigue during a sustained anaerobic test in well-trained cyclists. *Chronobiol. Int.* **2009**, *26*, 1622–1635. [CrossRef] [PubMed]
43. De Jonge, X.A.K.J. Effects of the Menstrual Cycle on Exercise Performance. *Sports Med.* **2003**, *33*, 833–851. [CrossRef]
44. International Organization for Standardization. *ISO 2631-1 Mechanical Vibration and Shock—Evaluation of Human Exposure to Whole-Body Vibration*; International Organization for Standardization: Geneva, Switzerland, 1997.
45. International Organization for Standardization. *ISO 5349-1 Mechanical Vibration—Measurement and Evaluation of Human Exposure to Hand-Transmitted Vibration*; International Organization for Standardization: Geneva, Switzerland, 2001.
46. Sacks, A.H. Theoretical Prediction of a Time-at-Pressure Curve for Avoiding Pressure Sores. *J. Rehabil. Res. Dev.* **1989**, *26*, 27–34.
47. Reswick, J.B.; Rogers, J.E. Experience at Rancho Los Amigos Hospital with devices and techniques to prevent pressure sores. In *Bed Sore Biomechanics*; Kenedi, R., Ed.; Palgrave: London, UK, 1976; pp. 301–310.
48. Hettinga, F.; De Konig, J.J.; de Vrijer, A.; Wust, R.C.I.; Daanen, H.A.M.; Foster, C. The effect of ambient temperature on gross-efficiency in cycling. *Eur. J. Appl. Physiol.* **2007**, *101*, 465–471. [CrossRef]

49. Maughan, R.J.; Otani, H.; Watson, P. Influence of relative humidity on prolonged exercise capacity in a warm environment. *Eur. J. Appl. Physiol.* **2012**, *112*, 2313–2321. [CrossRef]
50. Roa, S.; Doria, A.; Muñoz, L. Optimization of the bicycle weave and wobble modes. In Proceedings of the ASME 2018 IDETC Conference, Quebec City, QC, Canada, 26–29 August 2018. [CrossRef]
51. Bulsink, V.; Doria, A.; van de Belt, D.; Koopman, B. The effect of tyre and rider properties on the stability of a bicycle. *Adv. Mech. Eng.* **2015**, *7*, 1–19. [CrossRef]
52. Roa, S.; Muñoz, L. Bicycle change strategy for uphill time-trial races. *Proc. Inst. Mech. Eng. Part P J. Sports Eng. Technol.* **2017**, *231*, 207–219. [CrossRef]
53. Dahmen, T. Optimization of pacing strategies for cycling time trials using a smooth 6-parameter endurance model. In Proceedings of the 2012 Pre-Olympic Congress on Sports Science and Computer Science in Sport, Liverpool, UK, 24–25 July 2012.